Journal of New Materials for Electrochemical Systems 18, 137-143 (2015)

Investigations on Lithium Carbonate-alumina Composite Solid Electrolyte: Morphology and Related Conductivity

M. Sulaiman*, A.A. Rahman and N.S. Mohamed

Centre for Foundation Studies in Science, University of Malaya, 50603 Kuala Lumpur, Malaysia

Received: May 15, 2015, Accepted: July 25, 2015, Available online: September 30, 2015

Abstract: *Composite solid electrolytes in the system (1-x)Li_2CO_3-xAl_2O_3 with x = 0.1 – 0.6 mole were prepared via sol-gel technique. The morphology and conductivity of the composite were investigated. Obtained materials were analysed by X-ray diffraction, differential scanning calorimetry, scanning electron microscopy, Fourier transform infrared spectroscopy and chemical constituents were confirmed by energy dispersive X-ray. The ionic conductivity was measured using AC impedance spectroscopy. SEM studies of cross-section morphology clearly showed lithium carbonate crystals became radial – fluffy shaped particularly at x = 0.1 and 0.6. Morphological analysis showed homogeneous distribution between Li_2CO_3 and Al_2O_3 particles resulted in formation of amorphous phase of Li_2CO_3 at Li_2CO_3 - Al_2O_3 interface. Traces of α-$LiAlO_2$, γ-$LiAlO_2$ and $LiAl_5O_8$ were observed at x = 0.1, 0.2 and x = 0.4. Impedance spectroscopy studies showed that the conductivity is maximal at x = 0.2 and 0.4 - 0.5 with a value equal to ~10^{-3} Scm^{-1} with temperatures ranging from 130 - 180 °C.*

Keywords: Alumina composite; lithium carbonate; XRD; DSC; SEM; EDX

1. INTRODUCTION

Research on composite materials has been developed widely due to their solidity and simple form. A great diversity of applications are appraised such as solid state batteries, electrodes, fuel cells, sensors and other applications [1,2]. Many efforts have been devoted to develop solid-state secondary batteries; where lithium ion batteries are seen as power sources of choice due to its light weight, high voltage and high value of energy content. These properties triggered the growth of the market of electronic products [3]. Solid-state batteries have both solid electrodes and solid electrolytes where having good ion conductors will give a high power density to the system. For solid-state rechargeable lithium batteries, material with high Li^+ ion conductivity at room temperature is important [4]. Composite solid electrolyte component is the main of our study. In general, conductivity enhancement in composite can be explained by the presence of a great number of surfaces and interfaces, high mobile ion concentration, crystal structure, ionic polarizibility and other properties [1, 5-10]. In this work, composite solid electrolytes in the system (1-x)Li_2CO_3-$x$$Al_2O_3$ with x = 0.1 – 0.6 mole are prepared by sol-gel method. The conductivity enhancement of the composites is investigated. The structural characterizations are examined by X-ray diffraction, differential scanning calorimetry, scanning electron microscopy, Fourier transform infrared spectroscopy whereby ionic conductivity is measured by AC impedance spectroscopy. The aim of this paper is to report morphological features of the prepared composite samples corresponding to the conductivities ranging from ~10^{-3} to ~10^{-6} Scm^{-1} at 130 - 180 °C. We here in demonstrate that the conductivity of ~2×10^{-3} Scm^{-1} is high compared to the conductivity value of 1.05×10^{-6} Scm^{-1} at 250 °C in the same composite system prepared using conventional solid state sintering reported by Bhoga and Singh [11]. This means that the composite samples prepared in our sol-gel method are able to produce materials with a much higher ionic conductivity. It is our hope that the material can be employed in the future lithium rechargeable batteries.

*To whom correspondence should be addressed: Email: mazdidas@um.edu.my

2. EXPERIMENTAL

Composite system of (1-x)Li_2CO_3-$x$$Al_2O_3$ of x = 0.1 - 0.6 mole were synthesized by sol-gel method according to the procedure shown in the flow-chart (Fig. 1). Li_2CO_3 and Al_2O_3 (~10mm) of high purity grade were used as the starting materials. The powders of the samples were prepared by mixing the alumina powder of 0.1, 0.2, 0.3, 0.4, 0.5 and 0.6 moles in Li_2CO_3 in the presence of deionised water in a 500ml round bottomed flask. The solution

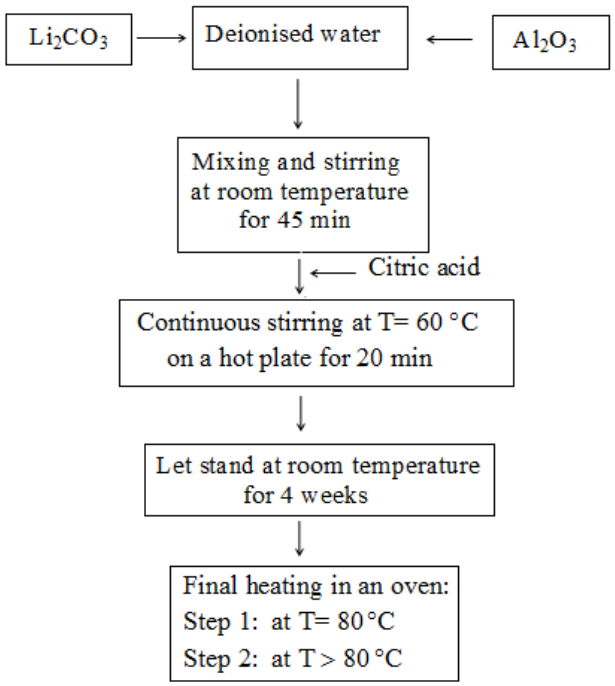

Figure 1. Flow chart of the synthesis procedure.

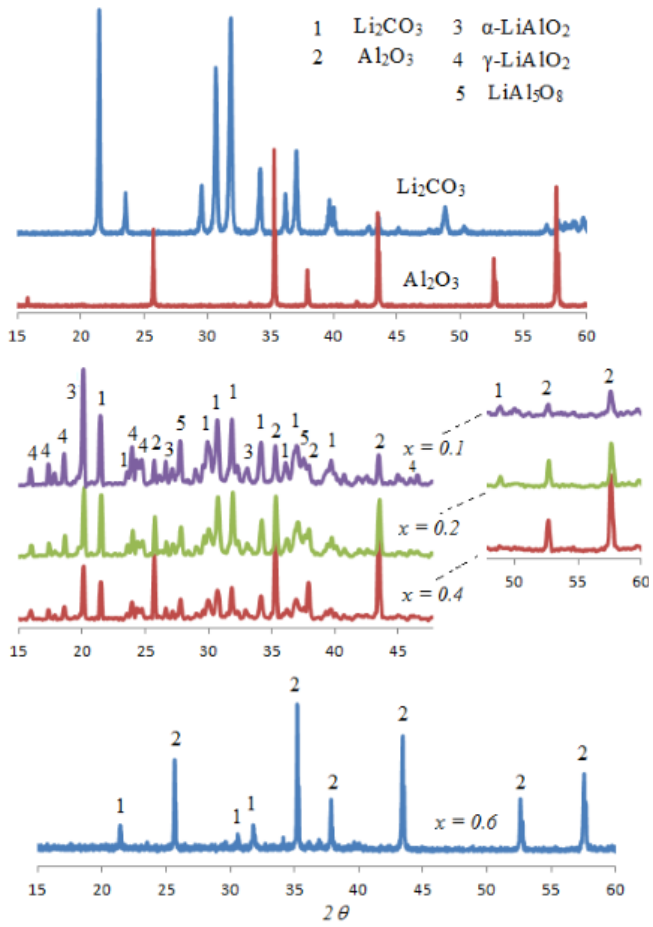

Figure 2. XRD patterns of Li_2CO_3, Al_2O_3 and (1-x)Li_2CO_3 – xAl_2O_3 composites.

was let under magnetic stirring at room temperature for 45 min. An equivalent mass of citric acid to the mass of alumina was added into the solution. The stirring process was continued for 20 min at 60 °C and left to stand at room temperature for four weeks. The mixture was gradually dried at 80 °C in an oven until a white gel was formed. In a next step, the gel was further heated until dry. A white powder was obtained as the final product after drying process and was milled into a fine powder in an agate mortar. Structural characterizations for XRD, FTIR and SEM/EDX were performed on a D8 Advanced-Bruker X-ray Diffractometer with Cu Kα radiation, a Perkin Elmer RX1 spectrometer and INCA Energy 200 (Oxford Ins.), respectively. The thermal properties of the samples were measured on a Mettler Toledo DSC 822 with continuous heating at a rate of 10 $^oC\ min^{-1}$. The ionic conductance measurements were performed on Solatron 1260 impedance analyzer [12].

3. RESULTS AND DISCUSSION

3.1. XRD analysis

Presented in Fig. 2 are XRD spectra of Li_2CO_3, Al_2O_3 and composite samples of (1-x)Li_2CO_3 – xAl_2O_3 . Pure Li_2CO_3 shows peaks at 2θ ~ 21°, 23.8°, 29.7°, 30.5°, 31.6°, 34°, 36°, 37°, 39.6° and 48.5°. As can be seen from the spectra, both Li_2CO_3 and Al_2O_3 compounds were present in all composite samples. The broadening of peaks and disappearance of Li_2CO_3 peaks at 2θ = 48.5° indicated the formation of the amorphous phase in all composite samples. A similar study has been reported in the literature [10]. The formation of the amorphous phase of Li_2CO_3 is owed to chemical and physical interactions of both Li_2CO_3 and Al_2O_3 phases. In the case of $LiNO_3$ and alumina, a similar explanation was reported by Neiman *et al* and Sulaiman *et al* [13,14]. At low content of Al_2O_3, the Li_2CO_3 coexist as crystalline and amorphous states [10]. It was shown that for composite samples with x = 0.1, 0.2 and 0.4, the Li_2CO_3 salt exists in these two states – crystalline and amorphous. A very low intensity of X-ray diffraction peaks associated to Li_2CO_3 crystalline salt was observed at x = 0.6. This indicated that at a high Al_2O_3 concentration, Li_2CO_3 salt is mainly in amorphous state.

Traces of crystalline of α-$LiAlO_2$, γ-$LiAlO_2$ and $LiAl_5O_8$ (lithium aluminates) were also formed in the composite samples prepared as indicated by weak peaks at 2θ ~ 15 - 29°, 33°, 38° and 47° [15] as shown in Fig. 2. The peaks were detected in the spectra of composite sample with x = 0.1, 0.2 and 0.4. The formation of these crystalline phases was the result of chemical and physical interactions of both Li_2CO_3 and Al_2O_3 crystalline phases. However, the diffraction patterns suggest that the growth of the crystal is blocked by the presence of the amorphous phase. The pathway of the crystallization of the lithium aluminates can be represented by the following route [16]:

Lithium carbonate + Alumina → Amorphous → α-$LiAlO_2$ → γ-$LiAlO_2$+$LiAl_5O_8$

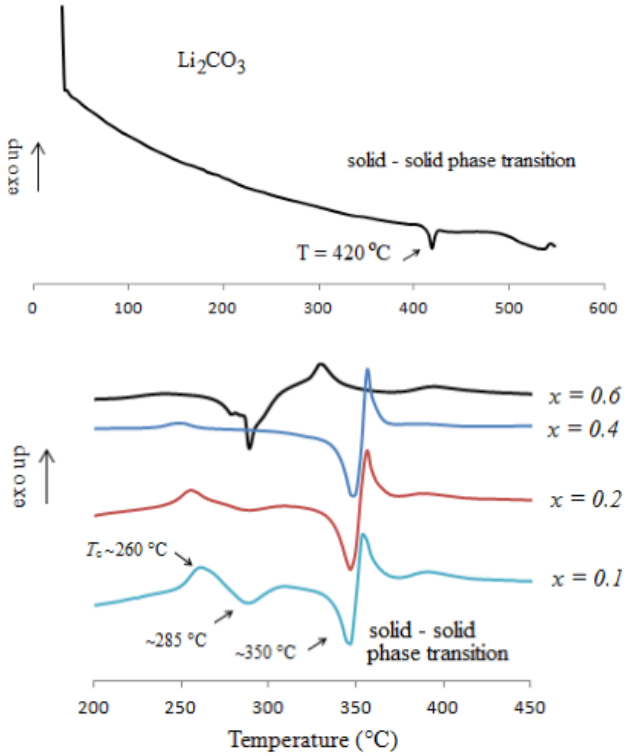

Figure 3. DSC curves of Li_2CO_3 and (1-x) $Li_2CO_3 - xAl_2O_3$ composites.

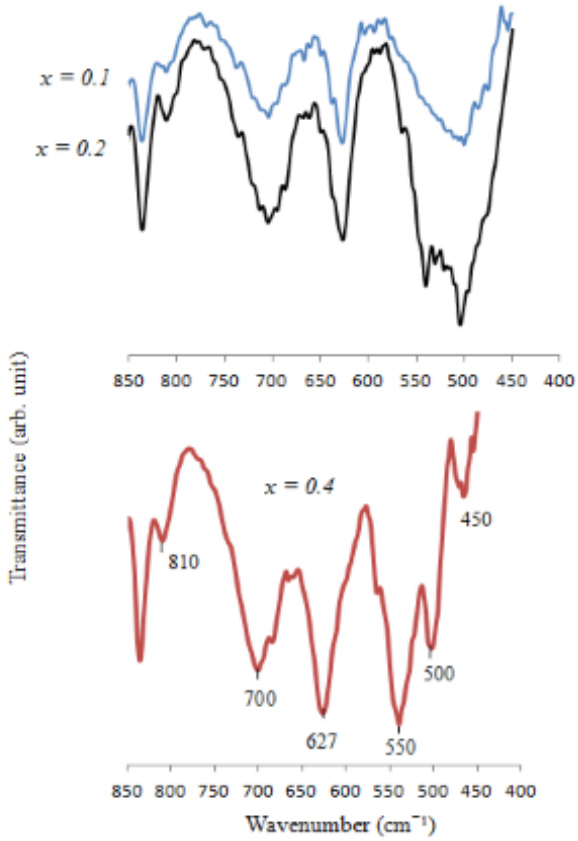

Figure 4. FTIR spectra of (1-x)$Li_2CO_3 - xAl_2O_3$ composites.

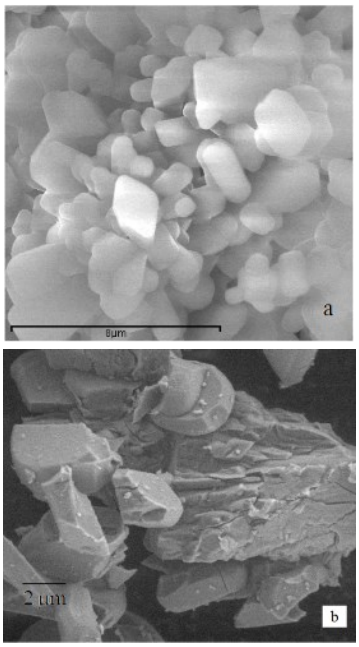

Figure 5. SEM micrographs of (a) pure Li_2CO_3 (8000×) and (b) pure Al_2O_3 (15000×).

3.2. DSC analysis

DSC curves of pure Li_2CO_3 and prepared composite samples are shown in Fig. 3. The solid-solid phase transition of Li_2CO_3 is observed at 420 °C [17]. For composite samples with x = 0.1, 0.2 and 0.4, the temperature of Li_2CO_3 phase transition has been lowered to ~350 °C due to the formation of amorphous phase as indicated by XRD results. At this point, both crystalline and amorphous states of Li_2CO_3 were present in the mixture. The amorphization of Li_2CO_3 salt is expected to occur with the increasing of alumina concentration. This effect was observed at x = 0.6 where the curve showed no solid-solid phase transition of Li_2CO_3 that would point to the present of crystalline phase.

Partial crystallization was observed in composite samples with x = 0.1, 0.2 and 0.4 with crystallization temperature, T_c ~260 °C. This exothermic peak was due to crystallization of α-$LiAlO_2$ which was identified by the XRD results. An endothermic peak ~285 °C was due to decomposition of α-$LiAlO_2$ and citric acid in the composite samples [18].

3.3. FTIR analysis

FTIR spectra of the composite samples are shown in Fig. 4. Peaks at 850 – 400 cm^{-1} are due to Al – O stretching vibrations in crystalline γ - $LiAlO_2$, γ – $LiAlO_2$ and $LiAl_5O_8$ formed in the samples [19]. Peaks at 810, 700, 627, 550, 500 and 450 cm^{-1} are associated with γ – $LiAlO_2$ and $LiAl_5O_8$ phases [20]. The FTIR results confirm their presence in the composite samples with x = 0.1, 0.2 and 0.4, as indicated by the XRD results.

3.4. SEM/EDX analysis

The SEM micrographs of pure ionic salt of Li_2CO_3 and Al_2O_3 are shown in Fig. 5. As can be seen, the Li_2CO_3 and alumina com-

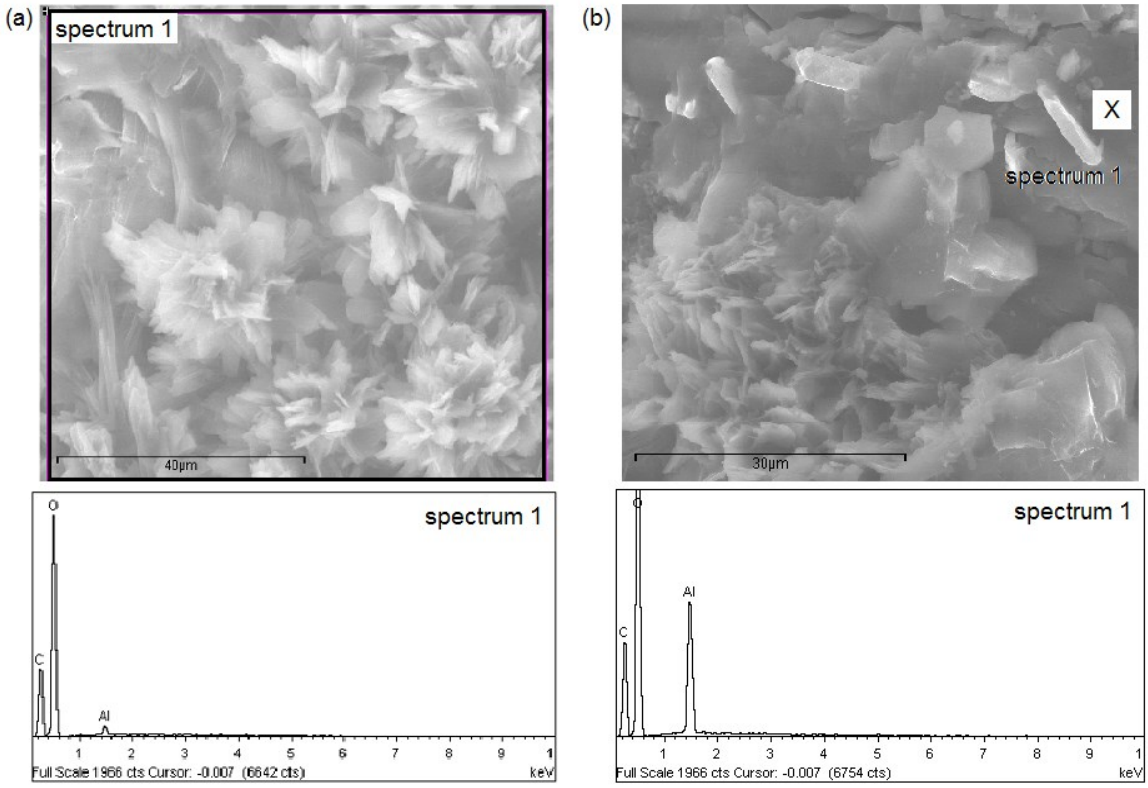

Figure 6. SEM/EDX spectra for composite sample with x = 0.1.

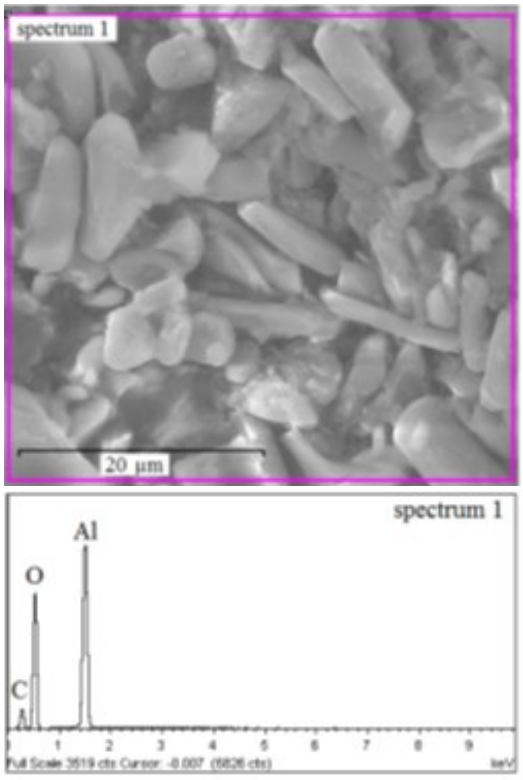

Figure 7. SEM/EDX spectra for composite sample with x = 0.2 (6000 X).

pounds present crystalline features; the Li_2CO_3 crystalline are broad columnar in shape with agglomeration whereby the alumina grains are spherical and flaky.

Figs. 6 and 7 show the cross-section morphology of composite samples with x = 0.1 and 0.2, respectively. The synthesis of composite solid electrolytes in the system $(1-x)Li_2CO_3$-xAl_2O_3 leads to the formation of a mixture of both amorphous and crystalline Li_2CO_3. In the case of the composite sample with x = 0.1, an amorphous phase together with traces of Li_2CO_3 crystalline can be seen (Fig. 6). From the SEM image, the Li_2CO_3 crystals grew radial – fluffy shapes in the presence of alumina particles. The morphology and the degree of agglomeration of Li_2CO_3 crystalline are transformed upon mixing with the alumina compound. This suggests that the sol-gel method employed in this work has affected the shape of the pure Li_2CO_3 crystals. The same phenomenon was reported by Watamura *et al* [21], whereby the shape and agglomeration of Li_2CO_3 changes prior treatment with other compound. The EDX spectra (Fig. 6) identify the chemical constituents of the composite sample with x = 0.1. The region selected with a square box shown in Fig. 6(a), evidenced the presence of C and O elements as major components implying the existence of Li_2CO_3 phase. The same elements are present in the second spectra (Fig. 6(b), marked by cross, X) that attributed to the amorphous phase of Li_2CO_3 as shown by the XRD results. The appearance of Al element is attributed to the Al_2O_3 phase.

Traces amount of lithium aluminates of α-$LiAlO_2$, γ-$LiAlO_2$ and $LiAl_5O_8$ are known to be formed following reaction between Li_2CO_3 and Al_2O_3 particles [12]. These lithium aluminates where in

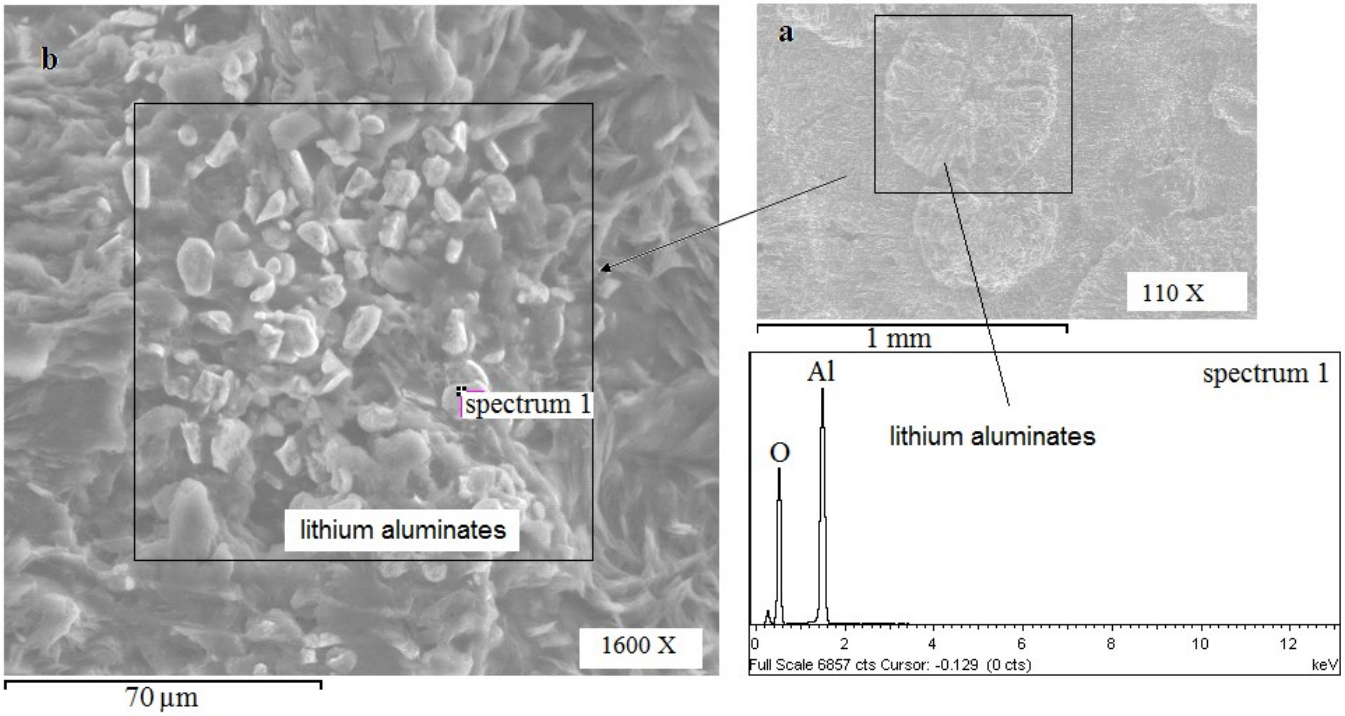

Figure 8. SEM/EDX spectra for composite sample with $x = 0.4$.

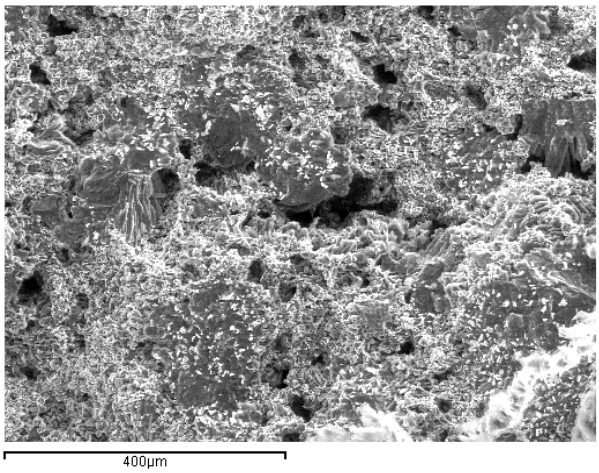

Figure 9. SEM micrograph (cross section) of composite sample with $x = 0.4$.

fact found in the composite samples with $x = 0.1$, 0.2 and 0.4 are further evidenced by the EDX analysis. For composite samples with $x = 0.2$ and 0.4, the presence of Al and O as major elements in the EDX spectra (Figs. 7 and 8), can be reasonably ascribed to the aforementioned lithium aluminates phases.

The surface microstructure of the composite sample with $x = 0.4$ in Fig. 8 showed the presence of particles of α-$LiAlO_2$, γ – $LiAlO_2$ and $LiAl_5O_8$ as confirmed by EDX analysis. At $x = 0.4$, the composite sample becomes slightly porous with pores size below 40 mm (Fig. 9). This fine porosity may very well facilitates the spreading of Li^+ cations throughout the materials enhancing thus ionic conductivity. At high content of alumina, the Li_2CO_3 particles are mainly in the amorphous state. At $x = 0.6$, one can observe, similarly to as the composite sample with $x = 0.1$; amorphous of Li_2CO_3 and alumina particles (Fig. 10).

Fig. 11 shows the morphology of the top surface of the composite samples with $x = 0.1$, 0.2 and 0.6. At $x = 0.1$, the surface is almost completely covered by the Li_2CO_3 phase. It can be clearly seen that the amount of Li_2CO_3 decreases as x increases. This is particularly obvious with $x = 0.6$. In addition, Li_2CO_3 particles are homogenously distributed with alumina particles. This homogenous distribution accounts for strong interfacial contact between alumina and Li_2CO_3 phases. This enhanced contact leads to the formation of amorphous phase of Li_2CO_3 and traces of lithium aluminates (α-$LiAlO_2$, γ-$LiAlO_2$ and $LiAl_5O_8$) as mentioned earlier.

3.5. Conductivity analysis

Scanning electron microscopic analysis of composite samples with $x = 0.1 – 0.6$, evidenced the systematic occurrence of an amorphous phase of Li_2CO_3 which results from physical and chemical interactions between crystalline Li_2CO_3 and Al_2O_3 particles [8,9,22,23]. It is here worth mentioning that the amorphous phase is responsible for enhancing the ionic conductivity of $(1-x)Li_2CO_3 – xAl_2O_3$ system because of Li_2CO_3 crystalline distortion that weakens ionic bonds [10,13]. Hence the number of free Li^+ ions increases, therefore facilitating ionic conduction. The effect of temperature on the conductivity of composite samples with $x = 0.1 – 0.6$ is given in Fig. 12. The conductivity is maximal at $x = 0.2$ and 0.4 - 0.5 with a value equal to $\sim 10^{-3}$ Scm^{-1} with temperatures ranging from 130 - 180 °C. From $x = 0.1$ to $x = 0.2$, the conductivity increases in a sigmoidal manner and decreases likewise beyond $x = 0.2$. The

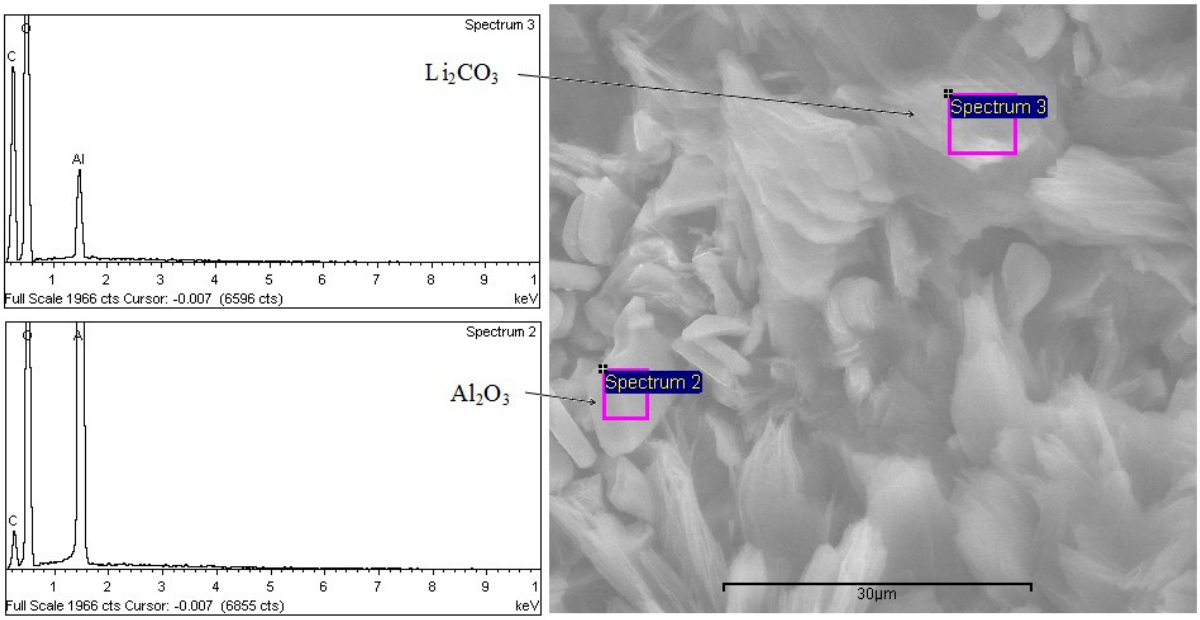

Figure 10. SEM/EDX spectra for composite sample with x = 0.6 (4000 X).

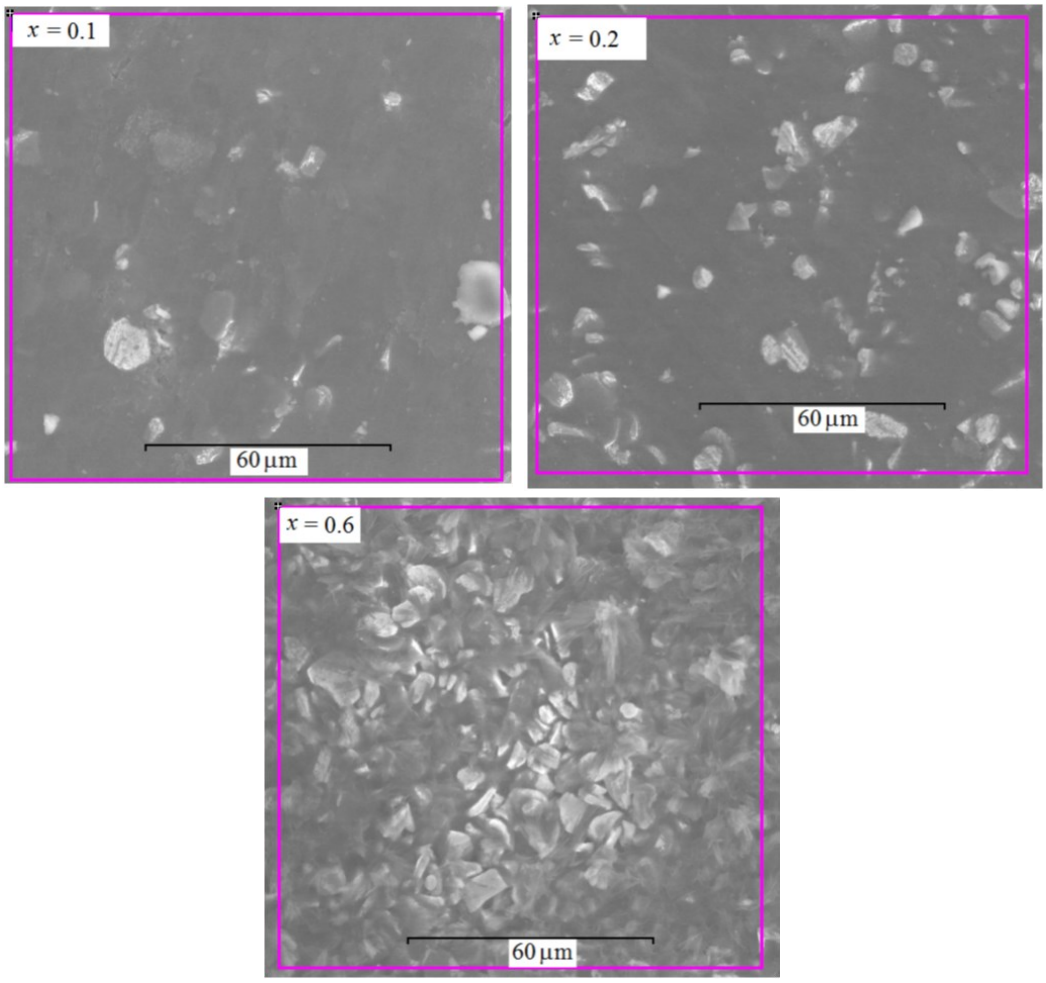

Figure 11. Top surface morphology of composite samples (2000 X).

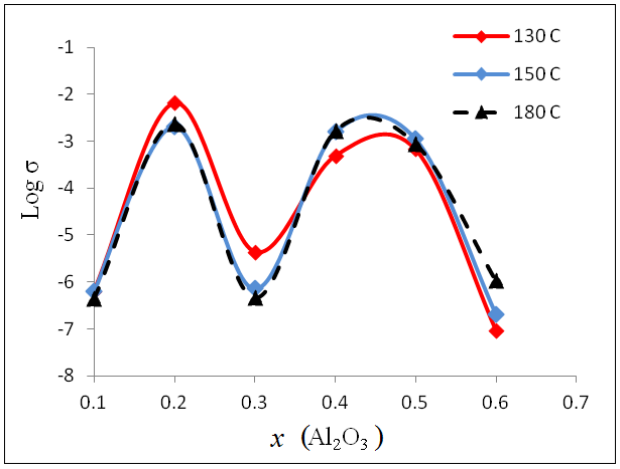

Figure 12. Conductivity versus alumina composition at different temperatures.

high conductivity observed at $x = 0.2$ is due to the formation of a new and highly conducting crystalline phase of lithium aluminates as reported in literatures [14,19,20]. Between $x = 0.3$ to $x = 0.4$ - 0.5, the conductivity increases again followed by a slight decrease beyond $x = 0.5$. The second episode of conductivity increment observed at $x = 0.4$ results from an increase of contact surface area between amorphous Li_2CO_3 and alumina due to the formation of micro pores in the composite material as suggested by our previous SEM analysis. The conductivity is further enhanced by the occurrence of crystalline particles (white phases) of α-$LiAlO_2$, γ – $LiAlO_2$ and $LiAl_5O_8$ which are uniformly dispersed in an amorphous matrix (dark area) as shown in Fig. 5. At $x = 0.6$, Al_2O_3 particles aggregate thus impeding the conductivity reaching in fact a value as low as ~10^{-6} Scm^{-1}. In sum, our study clearly demonstrates that the sol-gel method improves the ionic conductivity of Li_2CO_3–Al_2O_3 system as compared to the conventional solid state sintering proposed by Bhoga and Singh [11].

4. CONCLUSION

The present study demonstrates for the first time that the sol-gel method employed in the system $(1-x)Li_2CO_3$ $-xAl_2O_3$ yields an amorphous phase of Li_2CO_3 together with crystals of Li_2CO_3 with radial shapes. This was evidenced by XRD, DSC, SEM and EDX analysis. Further, interaction between Li_2CO_3 and alumina particles yielded traces of α-$LiAlO_2$, γ-$LiAlO_2$ and $LiAl_5O_8$ at $x = 0.1$, 0.2 and $x = 0.4$. Another demonstration is that the conductivity is enhanced firstly by amorphous Li_2CO_3 and secondly by the lithium aluminates. In order to improve the ionic conductivity, one could attempt to loosen further the ionic bond between Li^+ and CO_3^{2-} ions and further research in that direction is warranted.

5. ACKNOWLEDGMENT

The authors would like to thank the University of Malaya for granting the Research Grant (RG021/09AFR) to support this work.

REFERENCES

[1] J. Maier, Prog. Solid State Chem., 23, 171 (1995).
[2] J.B. Jr Wagner, Proceedings of the 6th International Conference on Solid State Ionics, Germany, 1987.
[3] B. Scrosati, J. Garche, J. Power Sources, 195, 2419 (2010).
[4] M. Tatsumisago, M. Nagao, A. Hayashi, J. Asian Ceramic Societies, 1, 17 (2013).
[5] J. Maier, J. Phys. Chem. Solids, 46, 309 (1985).
[6] J. Maier, Solid State Ionics, 75, 139 (1995).
[7] R.C. Agrawal, R.K. Gupta, J. Mater. Sci., 34, 1131 (1999).
[8] N.F. Uvarov, L.I. Brezhneva, E.F. Hairetdinov, Solid State Ionics, 136, 1273 (2000).
[9] N.F. Uvarov, E.F. Hairetdinov, B.B. Bokhonov, N.B. Bratel, Solid State Ionics, 86, 573 (1996).
[10] N. F. Uvarov, J. Solid State Electr., 15, 367 (2011).
[11] S.S. Bhoga, K. Singh, Solid State Ionics, 111, 85 (1998).
[12] M. Sulaiman, A.A. Rahman, N.S. Mohamed, Proceedings in 18th International Conference on Composite Materials, South Korea (2011).
[13] A.Y. Neiman, N.F. Uvarov, N.N. Pestereva, Solid State Ionics, 177, 3361 (2007).
[14] M. Sulaiman, N.A. Dzulkarnain, A.A. Rahman, N.S. Mohamed, Solid State Sci., 14, 127 (2012).
[15] R.B. Khomane, A. Agrawal, B.D. Kulkarni, Mater. Lett., 61, 4540 (2007).
[16] S.W. Kwon, S.B. Park, J. Nucl. Mater., 246, 131 (1997).
[17] K. Saito, K. Uchida, M. Tezuka, Solid State Ionics, 53, 791 (1992).
[18] M.A. Valenzuela, L. Téllez, P. Bosch, H. Balmori, Mater. Lett., 47, 252 (2001).
[19] M. Chatterjee, M.K. Naskar, J. Mater. Sci. Lett., 22, 1747 (2003).
[20] F. Oksuzomer, S.N. Koc, I. Boz, M.A. Gurkaynak, Mater. Res. Bull., 39, 71 (2004).
[21] H. Watamura, H. Marukawa, I. Hirasawa, J. Cryst Growth, 373, 111 (2013).
[22] G.V. Lavrova, V.G. Ponomareva, N.F. Uvarov, Solid State Ionics, 136, 1285 (2000).
[23] K. Tadanaga, K. Imai, M. Tatsumisago, T. Minami, J. Electrochem. Soc., 147, 4061 (2000).
[24] R.M. Biefield, R.T. Johnson, J. Solid State Chem., 29, 393 (1979).
[25] S. Hashimoto, K. Hattori, K. Inoue, A. Nakahashi, S. Honda, Y. Iwamoto, Mater. Res. Bull., 44, 70 (2009).